Carbohydrate Polymers 82 (2010) 887–894

Contents lists available at ScienceDirect

Carbohydrate Polymers

journal homepage: www.elsevier.com/locate/carbpol

Chain length effects on electrostatic interactions between hyaluronan fragments and albumin

Hélène Lenormand, Brigitte Deschrevel, Jean-Claude Vincent*

Laboratoire "Polymères, Biopolymères, Surfaces", FRE 3101 CNRS, Université de Rouen, 76821 Mont-Saint-Aignan cedex, France

ARTICLE INFO

Article history:
Received 29 March 2010
Received in revised form 26 May 2010
Accepted 7 June 2010
Available online 15 June 2010

Keywords:
Hyaluronan
Bovine serum albumin
Polysaccharide–protein complex
Chain length effect
Electrostatic interactions

ABSTRACT

We have shown that hyaluronan (HA) and bovine serum albumin (BSA) are able to form electrostatic HA–BSA complexes at pH 4, whatever the length of the HA chain over the very large domain ranging from 10^3 to 10^6 g mol^{-1}. Only the solubility of the HA–BSA complex depends on the HA chain length. The complex formation is optimum for HA chains of 50,000 g mol^{-1}. The stoichiometry is equal to 36 HA disaccharides per BSA molecule whatever the length of the HA chain may be. This suggests that the structure of the complex greatly depends on the HA chain length: a BSA molecule surrounded by several HA fragments for small HA chain length, and an HA molecule imprisoning several BSA molecules for high HA chain length. The HA chain length can thus control accessibility of the protein surface and eventually enzyme activity.

1. Introduction

Hyaluronan (HA) is a high-molar-mass polysaccharide composed of D-glucuronic acid-β(1,3)-N-acetyl-D-glucosamine disaccharide units linked together through β(1,4) glycosidic bonds. It is present in the extra cellular matrix (ECM) of connective, growing and tumour tissues where it is involved in cellular adhesion, mobility and differentiation (Catterall, 1995; Delpech et al., 1997; Girish & Kemparaju, 2007; Kennedy, Phillips, & Williams, 2002; Laurent, 1987; Rooney, Kumar, Ponting, & Wang, 1995). HA is the substrate of hyaluronidase (HAase). Three types of HAases exist, classified according to their cleavage mechanism (Meyer, 1971). In the human body, HAase is found in various organs (testis, skin, liver, kidney, uterus, etc.) and body fluids (plasma, sperm, urine, etc.). The testicular type HAases, which include human HAases and bovine testicular HAase, hydrolyse the glycosidic bonds in the β(1,4) position to produce HA of various chain lengths. It has been recently demonstrated that functions of HA strongly depend on the chain size (David-Raoudi et al., 2008; Stern, Asari, & Sugahara, 2006) and it appears that HA fragments and native HA may have opposite roles. For example, HA fragments of 2.5×10^5 g mol^{-1} induce the expression of genes involved in the inflammation process in macrophages (McKee et al., 1996, 1997) and in carcinoma cells (Fitzgerald, Bowie, Skeffington, & O'Neill, 2000), whilst native HA has an anti-inflammatory effect (Delmage, Powars, Jaynes, & Allerton, 1986; McBride & Bard, 1979). As generally, short HA oligosaccharides (4–25 disaccharides) have an angiogenic action (Rooney et al., 1995; West, Hampson, Arnold, & Kumar, 1985; West & Kumar, 1989) contrary to long HA chains (Deed et al., 1997), the ratio between high molecular weight HA and low molecular weight HA plays a role in cancer development (Mio & Stern, 2002; Stern, 2008). This ratio is at least partly controlled by the action of HAase (Cameron, 1966; Delpech et al., 1997; Mio & Stern, 2002).

In vitro, the action of HAase also depends on the HA chain length (Deschrevel, Tranchepain, & Vincent, 2008; Tranchepain, Deschrevel, & Vincent, 2005). We have studied the kinetics of native HA hydrolysis catalyzed by HAase (Astériou, Vincent, Tranchepain, & Deschrevel, 2006; Deschrevel, Lenormand, et al., 2008; Lenormand, Deschrevel, & Vincent, 2007, 2010; Lenormand, Tranchepain, Deschrevel, & Vincent, 2009; Vincent, Asteriou, & Deschrevel, 2003) using bovine testicular HAase as a model. By taking into account the shape of the numerous kinetic curves obtained under various experimental conditions, we have established that, whatever the experimental conditions, the experimental points of the HA hydrolysis kinetics can be perfectly fitted with a bi-exponential model. This has suggested that two different sets of kinetic parameters exist, according to the HA chain length (Vincent et al., 2003). We have thus studied the influence of the HA chain length on the kinetics of the HA hydrolysis catalyzed by bovine testicular HAase. For that purpose, and also in order to study the effect of HA chain length on biological processes (David-Raoudi et al., 2008), we have developed a method based on a kinetically

* Corresponding author at: Laboratoire "Polymères, Biopolymères Surfaces" CNRS UMR 6270 & FR 3038, Université de rouen, 76821 Mont Saint Aignan, France. Tel.: +33 2 35 14 67 42; fax: +33 2 35 14 67 04.
E-mail address: jean-claude.vincent@univ-rouen.fr (J.-C. Vincent).

0144-8617/$ – see front matter © 2010 Elsevier Ltd. All rights reserved.
doi:10.1016/j.carbpol.2010.06.011

controlled HA enzymatic hydrolysis to obtain HA fragments of the desired size with low polydispersity (Tranchepain et al., 2006). For the present study, 10-mg scale HA fragments with a molar mass ranging from 8×10^2 to 2.5×10^5 g mol^{-1} have been produced, purified by low pressure chromatography and characterised in molar mass by mass spectrometry and/or SEC-MALLS (size exclusion chromatography-multi-angle laser light scattering) chromatography (Tranchepain et al., 2006). The spectrophotometric method described by Reissig, Strominger, and Leloir (1955) and modified by Astériou et al. (2001), allowing the measurement of the molar concentration of N-acetyl-D-glucosamine reducing ends, has been used to follow the hydrolysis kinetics. Our studies (Deschrevel, Tranchepain, et al., 2008) have shown that HA_6 gives the lowest hydrolysis rate and that it is the worst substrate for the HAase-catalyzed hydrolysis. For short HA chain lengths, ranging from HA_6 to HA_{16} ($\log(M_n)$ between 3 and 3.5), the increase in the initial hydrolysis rate is mainly due to the strong decrease in K_m associated with the increase in V_m resulting from better interactions between the oligosaccharide and the enzyme. Nevertheless, the hydrolysis rate remains low because of the possible transglycosylation action mode of HAase. For middle HA fragments ranging from HA_{16} to HA_{300} ($\log(M_n)$ between 3.5 and 4.8), the initial hydrolysis rate is higher and its increase is related to a strong increase in V_m associated with a lower increase in K_m. The initial hydrolysis rate is maximum for HA_{300}. For long HA fragments ranging from HA_{300} to HA_{5000} ($\log(M_n)$ between 4.8 and 6), the slight decrease in the initial hydrolysis rate is produced by a decrease in V_m associated with an increase in K_m. Finally, two populations of HA fragments may be distinguished with respect to their hydrolysis rate: short HA oligosaccharides with a low hydrolysis rate and a mono-exponential kinetic shape (Deschrevel, Tranchepain, et al., 2008) resulting from transglycosylation and low stability of the enzyme–substrate complex (Vincent et al., 2003), and high HA chain length with a high hydrolysis rate and a bi-exponential kinetic shape resulting from high stability of the enzyme–substrate complex.

HAase activity is also controlled by the presence of non-catalytic proteins (Deschrevel, Lenormand, et al., 2008; Lenormand, Deschrevel, Tranchepain, & Vincent, 2008; Lenormand et al., 2009; Vincent & Lenormand, 2009) because of the electrostatic HA–protein complex formation and it is now of importance to learn more about the effect of the HA chain length on the HA–protein complex formation. The attractive forces between proteins and polysaccharides are essentially electrostatic with a possible contribution of hydrophobic and hydrogen interactions. When the electrostatic interactions are strong enough, they lead to the formation of complexes or coacervates which have been used for protein purification (Dubin, Gao, & Mattison, 1994) and immobilisation of active molecules (Kokufuta, 1992). Most of the experimental and theoretical work on protein–polysaccharide complexes has been reviewed by Cooper, Dubin, Kayimazer, and Turksen (2005) and Schmitt, Sanchez, Desobry-Banon, and Hardy (1998). The pertinent parameters controlling this type of complex include the concentrations of the biopolymers and their ratio (Xia & Dubin, 1994), the molar mass of the biopolymers (Wang, Kimura, Dubin, & Jaeger, 2000), but overall ionic strength (Burgess, 1990; Moss, Van Damme, Murphy, & Preston, 1997), pH (Burgess & Singh, 1993; Dubin et al., 1994) and temperature (Harding et al., 1993). Among these parameters, ionic strength is likely the most pertinent one to confirm or not the electrostatic nature of the interactions (Moss et al., 1997; Xu, Yamanaka, Sato, Miyama, & Yonese, 2000) which are strongest at very low, but not zero, ionic strength (Burgess, 1990) and decrease when ionic strength is increased by progressive screening of the charges borne by the biopolymers. Two main classes can be distinguished for the electrostatic complexes: (i) neutral insoluble complexes at the phase separation when the net positive charge of one of the biomacromolecules exactly compensates the net negative charge of the other, and (ii) charged complexes which are maintained in suspension by solvatation and can produce turbidity, when an excess of charge exists. Taglienti et al. (2006) have recently shown that interactions of HA polymers with proteins are based on surface polar interactions. Electrostatic complexes between native HA and proteins have been reviewed by Lenormand et al. (2008). Very interesting contributions have been brought by Xu et al. (2000) and Grymonpré, Staggemeier, Dubin, and Mattison (2001): Xu et al. have studied mixtures of native HA and BSA and showed both the electrostatic nature of the interactions between the two molecules and the strong influence of pH on the solubility of the HA–BSA complex. Grymonpré et al. focused particularly on the effects of both pH and ionic strength on the existence and solubility of the HA–BSA complexes.

There have been several reports showing that BSA enhances HAase activity (Gacesa, Savitsky, Dodgson, & Olavesen, 1981; Gold, 1980; Maingonnat et al., 1999). We have studied the enhancement–suppression of HAase activity by proteins and have shown that at low ionic strength and pH 4, HA and HAase, in addition to forming enzyme–substrate type complexes for the catalytic reaction, can form non-specific electrostatic complexes because HA is negative and HAase is positive (Deschrevel, Lenormand, et al., 2008; Lenormand et al., 2008). Although enzyme–substrate type complexes are stabilized by hydrogen bonds, electrostatic and Van der Waals interactions (Day & Sheehan, 2001), non-specific complexes are mainly stabilized by electrostatic interactions. It has also been shown that HAase is no longer catalytically active when complexed with HA only via electrostatic interactions (Astériou et al., 2006; Deschrevel, Lenormand, et al., 2008; Lenormand et al., 2007). HA–BSA complexes are able to compete with and dissociate HA–HAase complexes and thus are able to enhance HAase activity. This action is maximum at low ionic strength, but also occurs at physiological ionic strength (Lenormand et al., 2008).

Since then, we have studied in detail both the HA–BSA complexes with respect to the biomacromolecule concentrations at pH 4 (Lenormand et al., 2009) and their action on HAase activity with respect to pH (Lenormand et al., 2010) at low ionic strength. Whatever the parameter, pH or biomacromolecule concentrations, we have shown that three types of electrostatic complex can be distinguished depending on the charge of the complex. (i) Neutral insoluble complexes are obtained when the negative charge of HA is exactly compensated by the net positive charge of BSA. Insoluble complexes sediment by themselves, (ii) solubilized slightly charged complexes, when a small excess of charge exists; they produce turbidity and centrifugation causes their sedimentation in the pellet and (iii) solubilized highly charged complexes, when a great excess of charge exists; they may produce turbidity but centrifugation does not cause their sedimentation (Lenormand et al., 2009). Therefore, the typical scheme for HA–BSA complex formation, drawn as a function of any parameter, is characterised by the phase separation corresponding to insoluble complexes, surrounded by (i) the slightly charged complex region where complexes can be isolated in the centrifugation pellet, and then (ii) the highly charged complex region where complexes remain in the centrifugation supernatant. Calculations from experimental data have shown that insoluble complexes have an average charge excess lower than 5%, whilst centrifugation-driven sedimenting complexes have an average charge excess of about 10% and supernatant complexes have a higher charge excess reaching 30%. Because of the extraordinary importance of HA oligosaccharides (Stern et al., 2006) and the recent development of their industrial production, this raises the question of whether HA oligosaccharides are able to form complexes with BSA, preventing or reversing the formation of HA–HAase complexes and thus enhancing the HAase activity.

The present study of the interactions between HA oligosaccharides and BSA is particularly interesting since numerous proteins

that "specifically" interact with HA, the so-called hyaladherins, require only a small number of saccharides for recognition and binding. For example, hyaluronectin (HN) (Bertrand & Delpech, 1985), aggrecan core protein and link protein (Lapčík, Lapčík, De Smedt, Demeester, & Chabreček, 1998) need only a decasaccharide (approximately 2000 g mol^{-1}). That means that the binding between HA and these proteins does not occur when HA is shorter than a decasaccharide. Underhill (1992) showed that a hexasaccharide is long enough to bind to the CD44 cell receptor, but according to Tammi et al. (1998), HA bound to CD44 is displaced by HA_{10} and not by HA_6. Indeed, as shown by Lesley, Hascall, Tammi, and Hyman (2000), the complex involving HA_{10} and CD44 is more stable than that involving HA_6. A distinction should thus be made between the minimum chain length able to bind specifically to a protein (hyaladherin or HAase) and the chain length required to form a stable non-specific and efficient HA–protein complex. Other fundamental studies concerning the interactions between the G1-domain of versican and HA oligosaccharides have shown that this binding is cooperative (Seyfried, Day, & Almond, 2006) leading to the all-or-none model characterised by the simultaneous presence of fully complexed and free HA oligosaccharides. In a previous paper (Deschrevel, Tranchepain, et al., 2008) concerning the hydrolysis of oligosaccharides catalyzed by HAase, we have reported a large increase in the stability of the catalytic HA–HAase complex for HA chains ranging from HA_6 to HA_{16}, and in the rate constant for the formation of the complex for HA chains up to HA_{40}, with a lower increase for HA chains between HA_{40} and HA_{100}. The ability for HA chains longer than HA_{16} to form stable enzyme–substrate complexes, i.e. the ability to establish enough weak interactions with the enzyme, may be related to the fact that, unlike shorter size chains, these chains are long enough to be able to self-associate, thus forming dimer type structures by intermolecular interactions (Turner, Lin, & Cowman, 1988). Indeed, these results suggest that a minimum HA chain length is necessary for stable HA-HA as well as HA–protein associations to exist.

In fact, the electrostatic HA–BSA complex formation is characteristic of polyelectrolyte–polyelectrolyte interactions. What is the minimum HA chain length allowing complex formation with proteins and what is the nature of these complexes? The aim of this paper is to characterise the HA–protein, and especially the HA–BSA, complexes as a function of the HA chain length in order to learn more about the influence of the HA chain length on the HAase action in cancer. We do not examine the role of ionic strength in this paper and we only use low ionic strength conditions, which enhance electrostatic interactions. However, previous experiments (Lenormand et al., 2008) have shown that electrostatic complexes also exist at higher ionic strength. In order to more easily refer to our previous results with native HA, the present study is performed at pH 4 and low ionic strength.

2. Experimental

2.1. Materials

BSA (A 3675, lot 78H1399) and sodium HA from human umbilical cord (H 1876, lot 127H0482) were obtained from Sigma. The molar mass of native HA was close to 10^6 g mol^{-1}. More precisely, the number-average molar mass (M_n) of HA was 0.967×10^6 g mol^{-1} and its polydispersity index (Ip), which represents its degree of homogeneity, was 1.45. The HA fragments were obtained according to Tranchepain et al. (2006). The Ip value of all the produced HA fragments was smaller than 1.25, except for the fragment of 211,300 g mol^{-1} for which Ip was 1.45.

The molar mass of BSA was 69×10^3 g mol^{-1}. HA and BSA were used without any further purification. The chemicals used in the assays were: sodium tetraborate (Prolabo 27 727-297), sulfuric acid (Sigma S 1526), carbazole (Sigma C 5132), boric acid (Sigma B 7660), p-dimethylaminobenzaldehyde (DMAB) (Sigma D 8904), glacial acetic acid (Sigma A 6283).

Absorbance was measured using an Uvikon 860 KONTRON spectrophotometer equipped with a temperature-controlled chamber and connected to a computer. pH adjustments were carried out using a Metrohm 632 pH-meter equipped with a Radiometer Analytical XC161 pH electrode. Centrifugation of the HA–protein mixtures was performed with a MiniSpain Plus centrifuge from Eppendorf. Measurements of hydrodynamic diameters of HA–protein complexes were carried out using a Zeta Sizer (Nano ZS) from Malvern Instruments equipped with a laser source ($\lambda = 632$ nm). This apparatus was able to measure diameters of suspended particles ranging from 1 nm to 1 μm. Diameters of insoluble particles were not available.

2.2. Methods

2.2.1. Uronic acid assay

The HA fragment solution (weighed at 2 g L^{-1}) was prepared in Milli-Q water and assayed by the method described by Dische (1947) and modified by Bitter and Muir (1962). The method was extensively described in previous papers (Astériou et al., 2001; Vincent et al., 2003) and calibrated by using sodium glucuronate (Sigma G 8645).

2.2.2. Turbidity measurements

The solutions of HA fragments and BSA prepared in Milli-Q water were first adjusted to pH 4. The HA/BSA mixture was prepared by diluting adequate volumes of HA and BSA solutions in Milli-Q water so that the final concentrations were 0.2 g L^{-1} for HA and 1 g L^{-1} for BSA. The mixture was placed in the reactor maintained at 37 °C. Turbidity variation in time was measured at 400 nm in a spectrophotometer thermostated (37 °C) sample cell with a magnetic stirrer.

2.2.3. Analysis of the HA–protein complexes

The HA/BSA mixtures prepared in a tube were incubated at 37 °C under magnetic stirring for 30 min. Aliquots of 1 mL were removed, transferred to Eppendorf cones and centrifuged at 10,000 rpm for 20 min. The supernatant was removed and placed in a quartz cuvette in order to measure the BSA concentration at 280 nm by using the calibration curve previously established with BSA solutions of known concentrations. A 200 μL aliquot of the supernatant was then analysed using the uronic acid assay method in order to measure its HA content. Then, 1 mL of water containing 20 μL of KOH 2 mol L^{-1} was added to the pellet to obtain its complete dissolution. The concentrations of BSA and HA in the obtained solution were then measured using the same methods as above.

2.2.4. Measurement of the HA–protein complexes' size

Size measurements were performed with the HA/BSA mixtures at pH 4. The mixture was introduced into an appropriate plastic cuvette of 1 cm pathlength and placed in the Zeta Sizer. Three runs were performed per experiment. Results were expressed in percentage of light intensity scattered by the solution as a function of the diameter of the particles responsible for that scattering (Mattison & Kaszuba, 2004).

3. Results

3.1. Existence of the HA–BSA complexes

As for native HA (Lenormand et al., 2008), a series of experiments with HA fragments was performed at pH 4 because at this

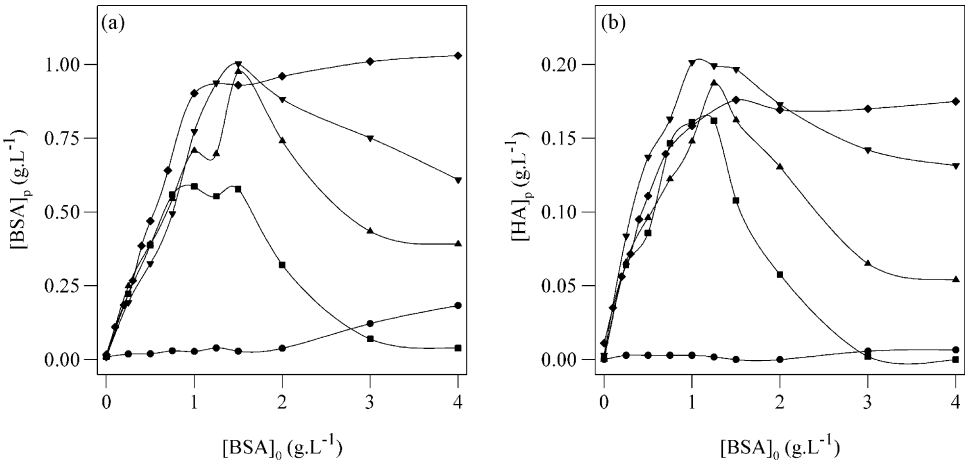

Fig. 1. Analysis of the composition of the electrostatic complexes formed between BSA and HA fragments. Distribution of BSA (a) and HA (b) in the pellet after centrifugation of mixtures composed of HA at 0.2 g L^{-1} and BSA at different concentrations ranging from 0 to 4 g L^{-1}, at pH 4 and low ionic strength (no added salt). Experiments were performed with different HA chain lengths: 2400 g mol^{-1} (●), 6800 g mol^{-1} (■), 9100 g mol^{-1} (▲), 17,000 g mol^{-1} (▼) and 10^6 g mol^{-1} (♦).

pH value, according to the p*I* value of BSA, estimated at 5.2 (Xu et al., 2000) and the pK_a value of HA, equal to 2.9 (Cleland, Wang, & Detweiler, 1982), the net positive charge of BSA allows the establishment of electrostatic interactions with HA whose net charge is negative. HA/BSA mixtures, with a 0.2 g L^{-1} HA fragment concentration and different BSA concentrations ($[BSA]_0$) ranging from 0.25 to 4 g L^{-1}, were prepared in Eppendorf tubes and incubated for 30 min at 37 °C. The HA samples were native HA and HA oligosaccharides of different molecular weights, 17,000, 9100, 6800 and 2400 g mol^{-1}. After centrifugation for 20 min at 10,000 rpm, the HA and BSA concentrations were measured in the pellet as described in Section 2.2. Fig. 1 shows the part of the BSA and HA concentrations present in the pellet as a function of the total BSA concentration $[BSA]_0$. This part corresponds to the neutral insoluble complexes plus the sedimentable slightly charged HA–BSA complexes. Fig. 1 shows that HA of 2400 g mol^{-1} molar mass did not form any sedimented complexes with low BSA concentrations (lower than 2 g L^{-1}). Conversely, the other HA oligosaccharides and the native HA formed sedimentable complexes with BSA. The HA and BSA contents of these complexes increased when the total BSA concentration $[BSA]_0$ was increased up to approximately 1.25 g L^{-1}. Then, the HA and BSA contents of the complexes decreased when the total BSA concentration was increased. The decrease was more pronounced for short HA oligosaccharides than for long HA oligosaccharides, and there was no decrease for native HA. That means that short HA oligosaccharides formed complexes with BSA only at low BSA concentrations. High BSA concentrations inhibited the HA–BSA complex formation. The optimal BSA concentration was between 1 and 1.5 g L^{-1}. This raises the question of whether HA oligosaccharides and BSA are able to form soluble complexes.

Fig. 2 shows the absorbance at 400 nm measured in the supernatants. As solubility of HA was higher than 10 g L^{-1} and that of BSA higher than 20 g L^{-1}, the presence of turbidity demonstrated the existence of HA–BSA coacervates. For all the HA fragments, turbidity was nil for $[BSA]_0$ ranging from 1 to 1.5 g L^{-1}; this corresponded to the maximum in sedimented HA–BSA complexes (Fig. 1). These conditions were close to those of the phase separation and all the HA–BSA complexes remained in the pellet; there was no soluble complexes. For the HA fragments of 9100 and 17,000 g mol^{-1} molar mass, turbidity was high both at lower $[BSA]_0$, between 0 and 1 g L^{-1}, and at higher $[BSA]_0$, between 1.5 and 4 g L^{-1}. This signifies that soluble highly charged HA–BSA complexes were formed over these two domains. For the HA fragments of 2400 and 6800 g mol^{-1} molar mass, turbidity only existed for $[BSA]_0$ higher than 1.5 g L^{-1}.

3.2. Kinetics of the HA–BSA complex formation

The optimal $[BSA]_0$ concentration for the formation of HA–BSA complexes was close to 1 g L^{-1} when the HA concentration was equal to 0.2 g L^{-1}. In order to examine the influence of HA chain length on the HA–BSA complex formation, a production of HA fragments of different chain lengths was performed according to the method developed by Tranchepain et al. (2006). The number-average molar mass (M_n) of the produced HA fragments were: 1200, 2400, 2700, 3900, 8400, 14,400, 20,000, 37,300, 53,000, 80,000, 211,000 and 1,000,000 g mol^{-1} (native HA). The HA–BSA complex formation was followed for 20 min by turbidity measurements at 400 nm, pH 4 and 37 °C; the HA fragment concentration was 0.2 g L^{-1} and the BSA concentration was 1 g L^{-1}. Fig. 3 shows

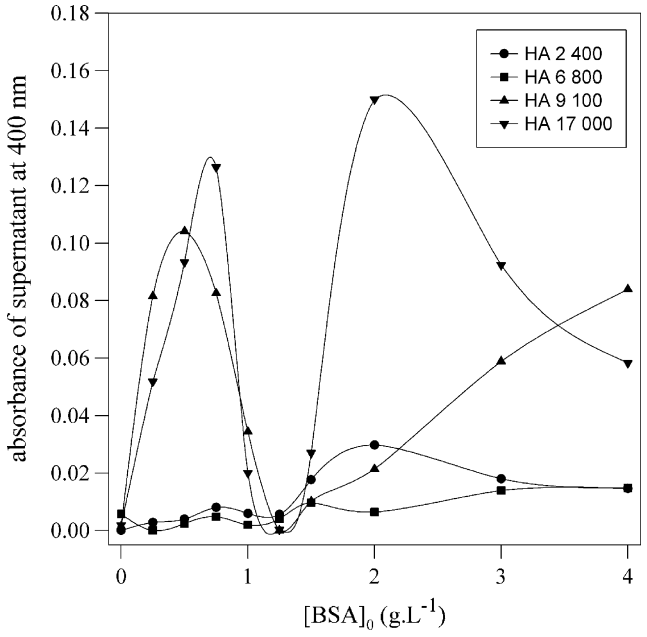

Fig. 2. Analysis of the composition of the HA–BSA complexes formed between BSA and HA fragments. Absorbance at 400 nm of the supernatant after centrifugation of mixtures composed of HA at 0.2 g L^{-1} and BSA at different concentrations ranging from 0 to 4 g L^{-1}, at pH 4 and low ionic strength (no added salt). Experiments were performed with different HA chain lengths: 2400 g mol^{-1} (●), 6800 g mol^{-1} (■), 9100 g mol^{-1} (▲) and 17,000 g mol^{-1} (▼).

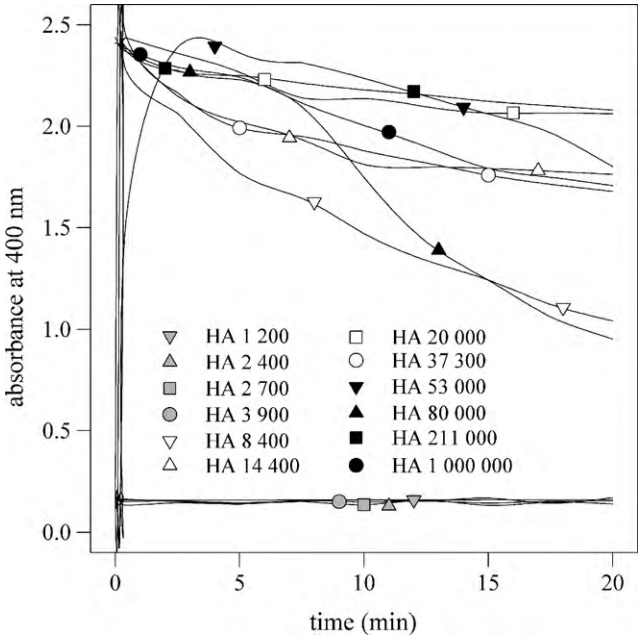

Fig. 3. Formation kinetics of the complexes formed between BSA and HA fragments. Time course of the absorbance at 400 nm of mixtures composed of HA at 0.2 g L^{-1} and BSA at 1 g L^{-1}, at pH 4 and low ionic strength (no added salt). Experiments were performed with different HA chain lengths ranging from 1200 to 10^6 g mol^{-1}.

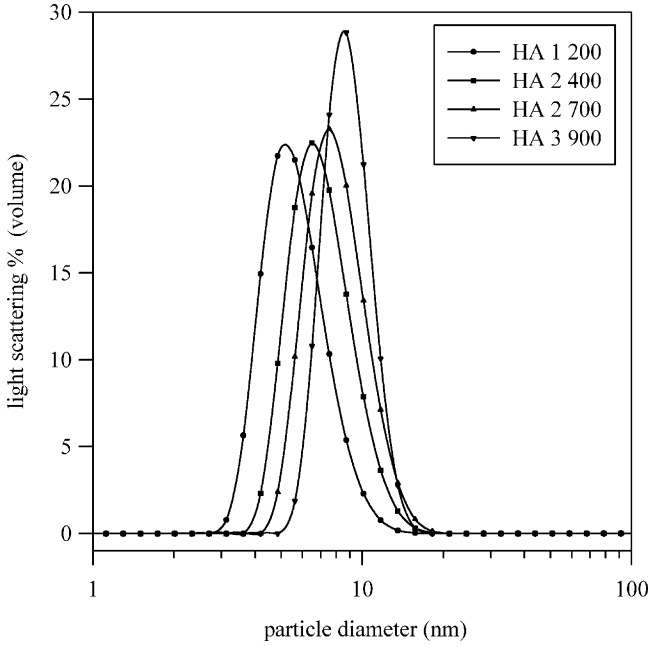

Fig. 4. Light scattering intensity of the HA–BSA complexes as a function of the particle diameter for different HA chain lengths: 1200 g mol^{-1} (●), 2400 g mol^{-1} (■), 2700 g mol^{-1} (▲) and 3900 g mol^{-1} (▼).

that turbidity remained extremely low for the four smallest HA fragments, suggesting either the absence of complexes or the presence of very small complexes. In fact, analysis of these solutions by using a Zeta Sizer showed that particles were formed and their diameter was ranging from 5 to 9 nm and increasing with the HA chain length (Fig. 4). This suggests that small soluble HA–BSA complexes were formed. For HA chain length higher than 3900 g mol^{-1} molar mass, kinetics showed a very fast increase in absorbance, followed by a slow decrease. This corresponds to the phase separation phenomenon: complex formation, aggregation of neutral complexes in large particles that fell down at the bottom of the tube, thus decreasing turbidity. Nevertheless, the fact that turbidity remained at a high level after 20 min showed that two types of complex were produced: a first type of HA–BSA complexes was neutral and sedimented and a second type was charged and remained in suspension causing turbidity.

3.3. Content of the HA–BSA complexes as a function of the HA chain length

As insoluble HA–BSA complexes remained at the bottom of the tubes, we analysed the composition of the liquid phase. The liquid phases of the previous mixtures were centrifuged and analysed for their HA and BSA content, according to Section 2.2. The assays allowed us to determine the HA and BSA concentrations in the supernatant and in the pellet. Fig. 5 shows the distribution of the BSA and HA concentrations between the supernatant, $[BSA]_s$ and $[HA]_s$, and the pellet, $[BSA]_p$ and $[HA]_p$, as a function of the HA chain length. In addition to these curves, the $[BSA]_i$ and $[HA]_i$, corresponding to the BSA and HA concentrations implicated in the insoluble complexes, were simply deduced by subtracting the concentrations corresponding to BSA and HA in the supernatant and in the pellet from the total BSA and HA concentrations. For HA chain lengths higher than 37,000 g mol^{-1} ($\log(M_n) > 4.5$),

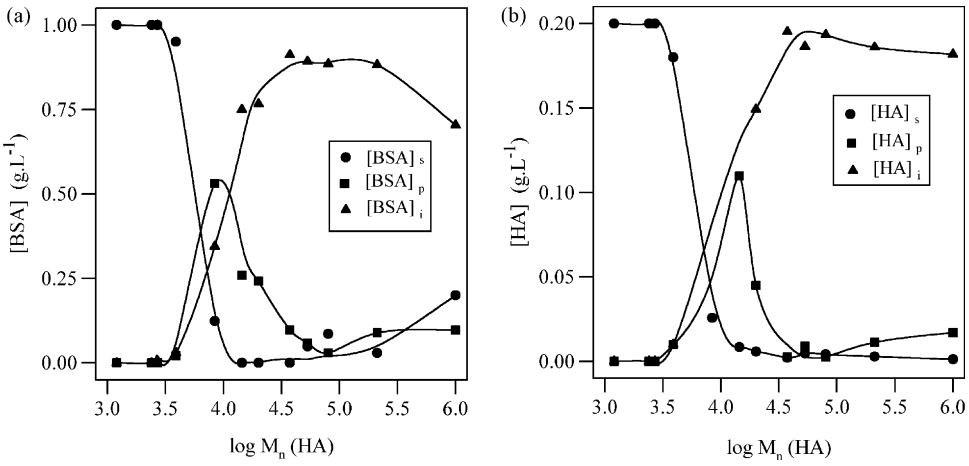

Fig. 5. Analysis of the composition of the electrostatic complexes formed between BSA and HA fragments. Distribution of BSA (a) and HA (b) as a function of the HA chain length (logarithmic scale) for the pellet (■), for the supernatant (●) and for the insoluble complexes (▲) after centrifugation of mixtures composed of HA at 0.2 g L^{-1} and BSA at 1 g L^{-1}, at pH 4 and low ionic strength (no added salt).

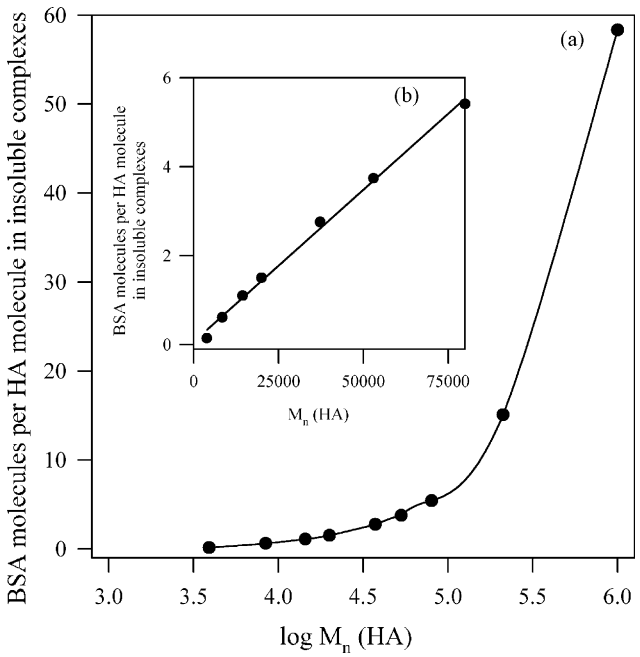

Fig. 6. Stoichiometry of the HA–BSA complexes expressed as the number of BSA molecules per HA molecule as a function of the HA chain length (logarithmic scale) for the pellet (including both slightly charged sedimentable and neutral insoluble complexes) after centrifugation of mixtures composed of HA at 0.2 g L^{-1} and BSA at 1 g L^{-1}, at pH 4 and low ionic strength (no added salt). The insert shows the same data in linear scale.

the major part of HA and BSA formed insoluble HA–BSA particles; between 4000 and 37,000 g mol^{-1} ($\log(M_n)$ ranged from 3.6 to 4.5), the insoluble and sedimentable slightly charged complexes were simultaneously predominant; for HA chain lengths smaller than 4000 g mol^{-1} ($\log(M_n) < 3.6$), the HA–BSA complexes were soluble. For very long HA chain length, higher than 211,000 g mol^{-1}, sedimentable slightly charged complexes were again present.

3.4. Stoichiometry of the HA–BSA complexes

Data presented in Fig. 5 were used to calculate the stoichiometry ϕ in the insoluble HA–BSA complexes. ϕ was defined as the number of BSA molecules per HA molecule:

$$\phi = \frac{N_{BSA}}{N_{HA}} = \frac{[BSA]_i / M_{BSA}}{[HA]_i / M_{n\,HA}}$$

Fig. 6 shows the stoichiometry ϕ as a function of the HA chain length in logarithmic scale (curve a), and in linear scale for the insert (curve b). Curve a shows that stoichiometry ϕ increased when the HA chain length was increased. Curve b (limited to 81,000 g mol^{-1}) shows a linear relationship between the number of BSA molecules per HA molecule and the molecular weight of the HA molecule. It means that the quantity of BSA, forming a complex with an HA molecule, was proportional to the molecular weight of that HA molecule, whatever the HA molecular weight. It was thus interesting to determine which HA chain length corresponded to one BSA molecule: the answer was 14,600 g mol^{-1}. In other words, 36 disaccharide units were complexed by one BSA molecule, whatever the molecular weight of the HA molecule. This stoichiometry has already been determined in systems containing native HA at 0.2 g L^{-1} and different BSA concentrations (Lenormand et al., 2008). The stoichiometry of the insoluble complexes was 38 disaccharides per BSA molecule, thus very similar to that determined here.

4. Discussion and conclusion

The most interesting conclusion of this study is that, at least at pH 4, HA and BSA are able to form electrostatic HA–BSA complexes whatever the length of the HA chain over the very large domain ranging from 10^3 to 10^6 g mol^{-1} ($\log(M_n)$ between 3 and 6). Even short HA oligosaccharides are able to form electrostatic complexes with BSA. Only the nature of the HA–BSA complexes depends on the HA chain length: highly charged soluble complexes for HA molar mass lower than 4000 g mol^{-1}, slightly charged sedimentable complexes for HA molar mass ranged between 4000 and 37,000 g mol^{-1}, neutral insoluble complexes for HA molar mass higher than 15,000 g mol^{-1}, with an optimum for 50,000 g mol^{-1}. For HA molar mass higher than 200,000 g mol^{-1}, slightly charged sedimentable and insoluble complexes are simultaneously present. The fact that HA–protein complexes are present over this large range of HA size is not, by itself, supporting the idea of using it for modulating HAase activity, since HA of different size might have opposite roles (see Section 1). However, solubility of HA–protein complexes, which is different and depends on the HA size may be involved in producing these different roles. As for example, HA–protein complexes are more soluble and weaker at low HA size than at high HA size. This likely leads to a modulation of HAase activity by proteins, lower at low HA sizes than at high HA sizes.

The present study has been conducted under given experimental conditions, in particular, pH and concentrations of HA and BSA. Previous experiments performed with native HA, i.e. with a molecular weight close to 10^6 g mol^{-1}, have shown that the nature of the HA–BSA complexes is dependent on the HA and BSA concentrations (Lenormand et al., 2008) and/or pH (Lenormand et al., 2010). It is likely that this double dependence also exists for complexes formed with HA fragments and the limits may be different from those previously found. For example, soluble complexes may exist at pH higher than 4, instead of insoluble complexes. Ionic strength is also a key parameter for the HA–BSA complex formation. The electrostatic interactions between HA and BSA are weaker when the ionic strength is increased. However, we have demonstrated the enhancement of the HAase activity by BSA, and thus the existence of the HA–HAase and HA–BSA complexes at pH 4 and physiological ionic strength (Lenormand et al., 2008).

HA–protein complexes have been used long ago in HAase assays based on the co-precipitation of long HA chains with proteins, as especially albumin, at acidic pH. When HA is hydrolysed by HAase, the precipitate disappears at a rate related to the HAase concentration. However, this Mucin Clot Prevention was only a qualitative method (Robertson, Ropes, & Bauer, 1940). An improvement of this method based on turbidimetry (Dorfman & Ott, 1948) was used during a long time to quantitatively assay HAase. The limit for turbidity was close to 7000 g mol^{-1}.

The second important conclusion concerns stoichiometry which is equal to 36 HA disaccharides per BSA molecule for the complexes isolated in the pellet under the experimental conditions used, i.e. pH 4 and HA and BSA concentrations fixed to 0.2 and 1 g L^{-1}, respectively. A previous study with native HA (Lenormand et al., 2008) has shown that complex stoichiometry ranged from 78 to 38 HA disaccharides per BSA molecule when 0 to 1 g L^{-1} of BSA were added to 0.2 g L^{-1} of native HA at pH 4. Calculations based on the charges borne by the two macromolecules, HA and BSA, have shown that the separation phase corresponding to the exact equality of positive and negative charges occurs for a stoichiometry of 44 HA disaccharides per BSA molecule. This study (Lenormand et al., 2008) has also shown that a stoichiometry of 38 HA disaccharides per BSA molecule corresponds to the slightly charged sedimentable HA–BSA complexes; this also corresponds to an HA molecule saturated with BSA molecules. The stoichiometry measured here was very close to that value. Another important result is that the stoi-

Fig. 7. Models for the different types of complex formed between HA and BSA as a function of the HA chain length: one BSA molecule surrounded by several HA fragments for small HA chain length; one HA molecule imprisoning several BSA molecules for high HA chain length; and one BSA molecule surrounded by one HA fragment for intermediate HA chain length.

chiometry, expressed as the number of HA disaccharides per BSA molecule in the complexes, remains constant whatever the HA chain length. This fact is very questionable since short HA fragments have not the same tri-dimensional structure as long HA molecules and can no longer be considered as polyelectrolytes. It is surprising that, at least concerning the charge equivalence, they behave exactly as polyelectrolytes. It is interesting to note that Courel et al. (2002) observed a similar chain length-dependence when studying the interactions between HA and hyaluronectin (HN), but the ratio between the quantity of HN complexed with HA and the HA chain length decreased between HA_{40} and HA_{100}.

The fact that the stoichiometry is constant whatever the HA chain length suggests that HA–BSA complexes may have different structures depending on the HA chain length. This constitutes the third conclusion of our study. For small HA chain length, the complex could be a spherical BSA molecule surrounded by several HA fragments in interaction with the positive charges borne by the BSA molecule. For high HA chain length, the complex could be an HA molecule imprisoning several spherical BSA molecules; the HA molecule being more compact when associated with proteins than the free HA molecule. There is an intermediate HA chain length for which one BSA molecule would be associated with one HA molecule. Because of the flexibility of the HA molecule, its persistence length and the size of the BSA molecule, it is possible to imagine a model where the HA molecule is around the BSA molecule (Fig. 7). It means that the HA chain length can control the accessibility of the protein surface and eventually the enzyme activity if the protein is an enzyme. This may contribute to the fact that HA molecules of different chain lengths may have different roles.

The studies performed with native HA have also shown that the electrostatic interactions leading to the HA–BSA complex formation are non-specific and can induce competition between proteins to form complexes with HA. The most interesting case concerns HAase, which is the natural enzyme for HA metabolism. HAase hydrolyses HA into oligosaccharides by forming a catalytic enzyme–substrate complex. Moreover, it can form electrostatic non-catalytic complexes with HA (Astériou et al., 2006; Deschrevel, Lenormand, et al., 2008; Lenormand et al., 2009, 2010; Vincent et al., 2003), but loses its catalytic activity when complexed to HA (Astériou et al., 2006; Deschrevel, Lenormand, et al., 2008). This produces an atypical kinetic behaviour, mainly characterised by an inhibition of the enzyme action at high substrate concentrations (Astériou et al., 2006; Lenormand et al., 2007; Vincent & Lenormand, 2009). The present study suggests that, as BSA, HAase should be able to form electrostatic complexes with HA fragments, whatever the HA chain length. As the structure of the HA fragment–BSA complexes greatly depends on the HA chain length, this raises the question of whether the HA fragment–HAase complexes are inactive or not. In the case of positive answer, which minimum HA chain length does make the HAase inactive. In this case, it is likely that BSA could prevent or reverse the HA–HAase complexes and enhance HAase activity, as for native HA. All of this could be important for the action of HAase in the ECM, in particular in the ECM of cancer cells, where long HA chains and short HA chains are present together and could be involved in inflammation processes and angiogenesis. This perspective may be quite far because present experimental conditions are different from the physiological conditions in the ECM. However, previous results with native HA have already shown that this type of electrostatic HA–protein complexes exist either at physiological ionic strength (Lenormand et al., 2008) or at physiological pH (Lenormand et al., 2010).

Acknowledgement

We thank Dr. Vishwas Purohit for critical readings of the manuscript.

References

Astériou, T., Deschrevel, B., Delpech, B., Bertrand, P., Bultelle, F., Merai, C., et al. (2001). An improved assay for the N-acetyl-D-glucosamine reducing ends of polysaccharides in the presence of proteins. *Analytical Biochemistry*, *293*, 53–59.

Astériou, T., Vincent, J. C., Tranchepain, F., & Deschrevel, B. (2006). Inhibition of hyaluronan hydrolysis catalysed by hyaluronidase at high substrate concentration and low ionic strength. *Matrix Biology*, *25*, 166–174.

Bertrand, P., & Delpech, B. (1985). Interaction of hyaluronectin with hyaluronic acid oligosaccharides. *Journal of Neurochemistry*, *45*, 434–439.

Bitter, T., & Muir, H. M. (1962). A modified uronic acid carbazole reaction. *Analytical Biochemistry*, *4*, 330–334.

Burgess, D. J. (1990). Practical analysis of complex coacervate systems. *Journal of Colloid and Interface Science*, *140*, 227–238.

Burgess, D. J., & Singh, O. N. (1993). Spontaneous formation of small sized albumin/acacia coacervate particles. *Journal of Pharmacy and Pharmacology*, *45*, 586–591.

Cameron, E. (1966). *Hyaluronidase and cancer*. Oxford: Pergamon.

Catterall, J. B. (1995). Hyaluronic acid, cell adhesion and metastasis. *Cancer Journal*, *8*, 320–324.

Cleland, R. L., Wang, J. L., & Detweiler, D. M. (1982). Polyelectrolyte properties of sodium hyaluronate. I. Salt exclusion in sodium chloride solution. *Macromolecules*, *15*, 382–386.

Cooper, C. L., Dubin, P. L., Kayimazer, A. B., & Turksen, S. (2005). Polyelectrolyte–protein complexes. *Current Opinion in Colloid and Interface Science*, *10*, 52–78.

Courel, M.-N., Maingonnat, C., Tranchepain, F., Deschrevel, B., Vincent, J. C., Bertrand, P., et al. (2002). Importance of hyaluronan length in a hyaladherin-based assay for hyaluronan. *Analytical Biochemistry*, *302*, 285–290.

David-Raoudi, M., Tranchepain, F., Deschrevel, B., Vincent, J. C., Bogdanowicz, P., Boumediene, K., et al. (2008). Differential effects of hyaluronan and its fragments on fibroblasts: Relation to wound healing. *Wound Repair and Regeneration*, *16*, 274–287.

Day, A. J., & Sheehan, J. K. (2001). Hyaluronan: Polysaccharide chaos to protein organisation. *Current Opinion in Structural Biology*, *11*, 617–622.

Deed, R., Rooney, P., Kumar, P., Norton, J. D., Smith, J., Freemont, A. J., et al. (1997). Early response gene signaling is induced by angiogenic oligosaccharides of hyaluronan in endothelial cells. Inhibition by nonangiogenic, high-molecular-weight hyaluronan. *International Journal of Cancer*, *71*, 251–256.

Delmage, J. M., Powars, D. R., Jaynes, P. K., & Allerton, S. E. (1986). The selective suppression of immunogenicity by hyaluronic acid. *Annals of Clinical and Laboratory Science*, *16*, 303–310.

Delpech, B., Girard, N., Bertrand, P., Courel, M.-N., Chauzy, C., & Delpech, A. (1997). Hyaluronan: Fundamental principles and applications in cancer. *Journal of Internal Medicine*, *242*, 41–48.

Deschrevel, B., Lenormand, H., Tranchepain, F., Levasseur, N., Astériou, T., & Vincent, J. C. (2008). Hyaluronidase activity is modulated by complexing with various polyelectrolytes including hyaluronan. *Matrix Biology*, *27*, 242–253.

Deschrevel, B., Tranchepain, F., & Vincent, J. C. (2008). Chain-length dependence of the kinetics of the hyaluronan hydrolysis catalyzed by bovine testicular hyaluronidase. *Matrix Biology*, *27*, 475–486.

Dische, Z. (1947). A new specific color reaction of hexuronic acid. *Journal of Biological Chemistry*, *167*, 189–198.

Dorfman, A., & Ott, M. (1948). A turbidimetric method for the assay of hyaluronidase. *Journal of Biological Chemistry*, *172*, 367–375.

Dubin, P. L., Gao, J., & Mattison, K. (1994). Protein purification by selective phase separation with polyelectrolytes. *Separation and Purification Methods*, *23*, 1–16.

Fitzgerald, K. A., Bowie, A. G., Skeffington, B. S., & O'Neill, L. A. (2000). Ras, protein kinase C zeta, and I kappa B kinases 1 and 2 are downstream effectors of CD44 during the activation of NF-kappa B by hyaluronic acids fragments in T-24 carcinoma cells. *Journal of Immunology*, *164*, 2053–2063.

Gacesa, P., Savitsky, M. J., Dodgson, K. S., & Olavesen, A. H. (1981). A recommended procedure for the estimation of bovine testicular hyaluronidase in the presence of human serum. *Analytical Biochemistry*, *118*, 76–84.

Girish, K. S., & Kemparaju, K. (2007). The magic glue hyaluronan and its eraser hyaluronidase: A biological overview. *Life Sciences*, *80*, 1921–1943.

Gold, E. W. (1980). An interaction of albumin with hyaluronic acid and chondroitin sulfate: A study of affinity chromatography and circular dichroism. *Biopolymers*, *19*, 1407–1414.

Grymonpré, K. R., Staggemeier, B. A., Dubin, P. L., & Mattison, K. W. (2001). Identification by integrated computer modeling and light scattering studies of an electrostatic serum albumin–hyaluronic acid binding site. *Biomacromolecules*, *2*, 422–429.

Harding, S., Jumel, K., Kelly, R., Gudo, E., Horton, J. C., & Mitchell, J. R. (1993). *The structure and nature of protein–polysaccharide complexes* (pp. 216–226). *Food proteins: Structure functionality*.

Kennedy, J. F., Phillips, G. O., & Williams, P. A. (2002). *Hyaluronan*. Wrexham, Wales: Woodhead Publishing.

Kokufuta, E. (1992). Functional immobilized biocatalysts. *Progress in Polymer Science*, *17*, 647–697.

Lapčík, L., Jr., Lapčík, L., De Smedt, S., Demeester, J., & Chabreček, P. (1998). Hyaluronan: Preparation, structure, properties, and applications. *Chemical Reviews*, *98*, 2663–2684.

Laurent, T. C. (1987). Biochemistry of hyaluronan. *Acta Oto-laryngologica (Supplement) (Stockholm)*, *442*, 7–24.

Lenormand, H., Deschrevel, B., Tranchepain, F., & Vincent, J. C. (2008). Electrostatic interactions between hyaluronan and proteins at pH 4: How do they modulate hyaluronidase activity. *Biopolymers*, *89*, 1088–1103.

Lenormand, H., Deschrevel, B., & Vincent, J. C. (2007). How electrostatic interactions can change the kinetic behaviour of a Michaelis–Menten enzyme. Application to the hyaluronane/hyaluronidase system. *Journal of Biological Physics and Chemistry*, *7*, 129–134.

Lenormand, H., Deschrevel, B., & Vincent, J. C. (2010). pH effects on the hyaluronan hydrolysis catalysed by hyaluronidase in the presence of proteins: Part I. Dual aspect of the pH-dependence. *Matrix Biology*, *29*, 330–337.

Lenormand, H., Tranchepain, F., Deschrevel, B., & Vincent, J. C. (2009). The hyaluronan–protein complexes at low ionic strength: How the hyaluronidase activity is controlled by the bovine serum albumin. *Matrix Biology*, *28*, 365–372.

Lesley, J., Hascall, V. C., Tammi, M., & Hyman, R. (2000). Hyaluronan binding by cell surface CD44. *Journal of Biological Chemistry*, *275*, 26967–26975.

Maingonnat, C., Victor, R., Bertrand, P., Courel, M.-N., Maunoury, R., & Delpech, B. (1999). Activation and inhibition of human cancer cell hyaluronidase by proteins. *Analytical Biochemistry*, *268*, 30–34.

Mattison, K. W., & Kaszuba, M. (2004). Molecular weight measurements with the zetasizer nano system. *American Biotechnological Laboratory*, *23*, 1–6.

McBride, W. H., & Bard, J. B. (1979). Hyaluronidase sensitive halos around adherent cells. Their role in blocking lymphocyte-mediated cytolysis. *Journal of Experimental Medicine*, *149*, 507–515.

McKee, C. M., Lowenstein, C. J., Horton, M. R., Wu, J., Bao, C., Chin, B. Y., et al. (1997). Hyaluronan fragments induce nitric-oxide synthase in murine macrophages through a nuclear factor NF-κB-dependent mechanism. *Journal of Biological Chemistry*, *272*, 8013–8018.

McKee, C. M., Penno, M. B., Cowman, M., Burdick, M. D., Strieter, R. M., Bao, C., et al. (1996). Hyaluronan (HA) fragments induce chemokine gene expression in alveolar macrophages. The role of HA size and CD44. *Journal of Clinical Investigation*, *98*, 2403–2413.

Meyer, K. (1971). Hyaluronidases. In P. D. Boyer (Ed.), *The enzymes* (pp. 307–320).

Mio, K., & Stern, R. (2002). Inhibitors of the hyaluronidases. *Matrix Biology*, *21*, 31–37.

Moss, J., Van Damme, M.-P., Murphy, W., & Preston, B. (1997). Dependence of salt concentration on glycosaminoglycan–lysozyme interactions in cartilage. *Archives of Biochemistry and Biophysics*, *348*, 49–55.

Reissig, J., Strominger, J., & Leloir, J. (1955). A modified colorimetric method for the estimation of N-acetylamino sugars. *Journal of Biological Chemistry*, *217*, 959–966.

Robertson, W., Ropes, M., & Bauer, W. (1940). Mucinase: A bacterial enzyme which hydrolyzes synovial fluid mucin and other mucins. *Journal of Biological Chemistry*, *133*, 261–276.

Rooney, P., Kumar, S., Ponting, J., & Wang, M. (1995). The role of hyaluronan in tumour neovascularization. *International Journal of Cancer*, *60*, 632–636.

Schmitt, C., Sanchez, C., Desobry-Banon, S., & Hardy, J. (1998). Structure and technofunctional properties of protein–polysaccharide complexes: A review. *Critical Reviews in Food Science and Nutrition*, *38*, 689–753.

Seyfried, N. T., Day, A. J., & Almond, A. (2006). Experimental evidence for all-or-none cooperative interactions between the G1-domain of versican and multivalent hyaluronan oligosaccharides. *Matrix Biology*, *25*, 14–19.

Stern, R. (2008). Hyaluronidases in cancer biology. *Seminars in Cancer Biology*, *18*, 275–280.

Stern, R., Asari, A. A., & Sugahara, K. N. (2006). Hyaluronan fragments: An information-rich system. *European Journal of Cell Biology*, *85*, 699–715.

Tammi, R., MacCallum, D., Hascall, V. C., Pienimäki, J.-P., Hyttinen, M., & Tammi, M. (1998). Hyaluronan bound to CD44 on keratinocytes is displaced by hyaluronan decasaccharides and not hexasaccharides. *Journal of Biological Chemistry*, *273*, 28878–28888.

Taglienti, A., Cellesi, F., Crescenzi, V., Sequi, P., Valentini, M., & Tirelli, N. (2006). Investigating the interactions of hyaluronan derivatives with biomolecules. The use of diffusional NMR techniques. *Macromolecular Bioscience*, *6*, 611–622.

Tranchepain, F., Deschrevel, B., Courel, M.-N., Levasseur, N., Le Cerf, D., Loutelier-Bourhis, C., et al. (2006). A complete set of hyaluronan fragments obtained from hydrolysis catalyzed by hyaluronidase: Application to studies of hyaluronan mass distribution by simple HPLC devices. *Analytical Biochemistry*, *348*, 232–242.

Tranchepain, F., Deschrevel, B., & Vincent, J. C. (2005). Influence of the chain length of hyaluronan on the kinetics of its hydrolysis catalyzed by hyaluronidase. In E. A. Balazs, & V. C. Hascall (Eds.), *Hyaluronan: Structure, metabolism, biological activities, therapeutic applications* (pp. 247–252). Matrix Biology Institute.

Turner, R. E., Lin, P., & Cowman, M. K. (1988). Self-association of hyaluronate segments in aqueous NaCl solution. *Archives of Biochemistry and Biophysics*, *265*, 484–495.

Underhill, C. (1992). CD44: The hyaluronan receptor. *Journal of Cell Science*, *103*, 293–298.

Vincent, J. C., Asteriou, T., & Deschrevel, B. (2003). Kinetics of hyaluronan hydrolysis catalysed by hyaluronidase. Determination of the initial reaction rate and the kinetic parameters. *Journal of Biological Physics and Chemistry*, *3*, 35–44.

Vincent, J. C., & Lenormand, H. (2009). How hyaluronan–protein complexes modulate the hyaluronidase activity: The model. *Biophysical Chemistry*, *145*, 126–134.

Wang, Y., Kimura, K., Dubin, P. L., & Jaeger, W. (2000). Polyelectrolyte–Micelle coacervation: Effects of micelle surface charge density, polymer molecular weight, and polymer/surfactant ratio. *Macromolecules*, *33*, 3324–3331.

West, D. C., Hampson, I. N., Arnold, F., & Kumar, S. (1985). Angiogenesis induced by degradation products of hyaluronic acid. *Science*, *228*, 1324–1326.

West, D. C., & Kumar, S. (1989). Hyaluronan and angiogenesis. In D. Evered, & J. Whelan (Eds.), *The biology of hyaluronan* (pp. 187–207). Chichester: John Wiley and Sons.

Xia, J., & Dubin, P. L. (1994). Protein–polyelectrolyte complexes. In P. L. Dubin, J. Bock, R. Davis, D. N. Schulz, & C. Thies (Eds.), *Macromolecular complexes in chemistry and biology* (pp. 247–271). Berlin: Springer Verlag.

Xu, S., Yamanaka, J., Sato, S., Miyama, I., & Yonese, M. (2000). Characteristics of complexes composed of sodium hyaluronate and bovine serum albumin. *Chemical and Pharmaceutical Bulletin*, *48*, 779–783.